Volume-activated Chloride Currents from Human Fibroblasts: Blockade by Nimodipine

M. K. Chung[1] and H. Ch. Kim[1,2]

1 *Department of Physiology, School of Dentistry and Institute of Oral Biology, Kyung Hee University, Seoul, Korea*
2 *East-West Medical Research Institute, Kyung Hee University, #1, Hoeki-Dong, Dongdaemun-Ku, Seoul 130–701, Korea*

Abstract. The whole-cell patch clamp technique was used to identify and to characterize volume-activated Cl^- current ($I_{Cl(vol)}$) in fibroblasts derived from human periodontal ligament. During osmotic cell swelling, the cells exhibited an outwardly rectifying current, which was dependent upon the concentration of external Cl^-. The anion permeability sequence of the chloride channel for anions was as follows: $SCN^- > I^- > Br^- > Cl^- > F^-$ > methanesulphonate > gluconate. Being an inhibitor of Cl^- channels and Cl^-/HCO_3^- exchanger, 4,4'-diisothiocyanato-stilbene-2,2'-disulfonic acid (DIDS) inhibited the currents with a voltage-dependence (EC_{50} = 57 μmol/l at +80 mV), and 5-nitro-2-(3-phenylpropylamino)-benzoic acid (NPPB), a carboxylate analogue Cl^- channel blocker, showed the reversible suppression of the currents in a dose-dependent manner (EC_{50}= 59 μmol/l). Nimodipine, a selective dihydropyridine Ca^{2+} channel blocker suppressed $I_{Cl(vol)}$ (EC_{50} = 66 μmol/l) and the effects were quite similar to those of NPPB. Nifedipine, another DHP blocker also inhibited the currents but with lesser efficacy (EC_{50} = 139 μmol/l). The removal of external Ca^{2+} or the addition of Cd^{2+} in the bath solution did not affect the blocking effects of nimodipine on $I_{Cl(vol)}$. These findings demonstrate that the human fibroblasts $I_{Cl(vol)}$ was suppressed by nimodipine in an extracellular Ca^{2+}-independent way. These results may provide, at least in part, an explanation for the Ca^{2+}-independent decrease in Cl^-/organic osmolytes efflux and RVD responses by nimodipine in some cell types.

Key words: Chloride current — Nimodipine — Fibroblasts

Introduction

Volume-activated Cl^- currents ($I_{Cl(vol)}$) have been described in numerous cell types (Kubo and Okada 1992; Gosling et al. 1995; Nilius et al. 1997), and are known to

Correspondence to: Hyung-Chan Kim, DDS, MS, PhD., Department of Oral Physiology, School of Dentistry and Institute of Oral Biology, Kyung Hee University, #1, Hoeki-Dong, Dongdaemun-Ku, Seoul 130–701, Korea. E-mail: chan@nms.kyunghee.ac.kr

be responsible for osmotically active particles efflux, including organic osmolytes as well as Cl^-, during cell swelling leading in many cells to regulatory volume decrease (RVD) responses (Okada 1997). Although there are a few minor differences, $I_{Cl(vol)}$ show generally (1) an outwardly rectifying current-voltage (I-V) relationship, (2) inactivation at depolarization, (3) inhibition by common Cl^- channel blockers, and (4) insensitivity to changes in cytoplasmic Ca^{2+} concentration (Nilius et al. 1996).

Nimodipine, a dihydropyridine (DHP) Ca^{2+} channel blocker, was reported to be able to inhibit the efflux of osmolytes and RVD responses in several cell types (O'Connor and Kimelberg 1993; Sánchez-Olea et al. 1995; Morán et al. 1997a,b). In astrocytes (O'Connor and Kimelberg 1993), the mechanism was suggested to involve the blockade of L-type Ca^{2+} channels, reducing the Ca^{2+}-activated K^+ and Cl^- conductances responsible for the efflux of intracellular osmolytes. However, Ca^{2+}-independent inhibition of the RVD by nimodipine was also reported in some other cells, such as cerebellar granule neurons (Morán et al. 1997b), fibroblasts (Morán et al. 1997a; Pasantes-Morales et al. 1997), and even in astrocytes (Sánchez-Olea et al. 1995). In those preparations, the effects of nimodipine were not changed in the absence of extracellular Ca^{2+}, and other Ca^{2+} channel blockers showed negligible effects on the osmolytes efflux and RVD. Based on these reports, it can be postulated that both the Ca^{2+}-independent effects of nimodipine on the Cl^-/amino acid efflux decreasing and the inhibition of RVD under hypotonic condition may be resulted from blockade of any pathway (s) responsible for Cl^- and/or organic osmolytes, e.g., volume-activated Cl^- channels.

In the present study we characterized the $I_{Cl(vol)}$ in human fibroblasts, tested the effects of nimodipine on $I_{Cl(vol)}$, and investigated any possible involvement of extracellular Ca^{2+} in the effects of nimodipine. The results showed that nimodipine suppressed $I_{Cl(vol)}$ efficiently in an extracellular Ca^{2+}-independent way.

Materials and Methods

Cell cultures

Human fibroblasts were obtained from human periodontal ligament explants dissected from the mid-root of four fully erupted premolar teeth according to the methods described by Somerman et al. (1989). The teeth were placed in sterile Dulbecco's modified Eagle's medium (DMEM) immediately after extraction. Under sterile conditions, the periodontal ligament tissue was mechanically removed and placed in 35-mm plastic tissue culture plates (Falcon) which contained culture medium composed of DMEM, 10% heat-inactivated fetal bovine serum, 100 units/ml penicillin, and 100 μg/ml streptomycin. The cells from the explant were allowed to proliferate undisturbed for 2–3 weeks in humidified 5% CO_2 incubator at 37℃. Trypsin-EDTA incubation was used to remove the cells, which were then transferred into 100-mm plastic tissue culture plates (Falcon) for continued growth. These cells were maintained in the same culture medium and passed as needed for the experimentation. For electrophysiological studies, the cells of passage 3–8 were

plated onto a sterile untreated glass coverslip at 1×10^4 cells ml^{-1} and used after 2–7 hours of incubation when the cells were still roundish.

Electrophysiology

Patch clamp pipettes were manufactured from thin-walled soda lime glass (1.2-mm o.d.), using a two-stage vertical pipette puller (L/M-3P-A, List Electronics), and were fire-polished using a microforge (MF-83, Narishige). Because of large currents, low-resistance pipettes (around 0.75–1.5 MΩ when filled with a CsCl-based pipette solution) were employed to reduce the voltage drop across the residual series resistance. Cell membrane capacitance was estimated from the amplifier setting required to neutralize the capacitive transient evoked by 5 mV voltage-step pulses. Mean membrane capacitance was 13.1 ± 0.5 pF ($n = 120$). The bath was grounded using an Ag-AgCl electrode through a 1 mol/l CsCl agar bridge to minimize the changes in liquid junction potentials with various external solutions and membrane potentials were corrected for liquid junction potentials as described by Neher (1992). Leak currents were not subtracted and all current values were plotted as absolute values measured with respect to the zero current level. The whole-cell patch clamp recording (Hamill et al. 1981) was performed with an Axopatch 200 A patch clamp amplifier (Axon Instrument) connected to a digital computer through a Labmaster (PP-50) DMA interface (Scientific Solution). Voltage-step protocols were generated, and data were acquired and analysed using an IBM-AT compatible computer and pCLAMP 6.0 software (Axon Instrument). All experiments were performed at room temperature (22–25 ℃).

Experimental solutions

External and internal solutions were designed to enhance the I_{Cl} recording. In order to minimize the cationic currents activated by either voltage or Ca^{2+}, CsCl and 1 mmol/l EGTA were added into the pipette solution. The pipette solution consisted of 140 CsCl, 1.2 $MgCl_2$, 1 EGTA, 10 HEPES, 5 D-mannitol, 2 Na_2-ATP (in mmol/l, pH 7.4, 300–310 mosmol/l). The composition of isotonic bath solution was as follows (in mmol/l): 140 CsCl, 0.5 $MgCl_2$, 1.3 $CaCl_2$, 10 HEPES, 20 D-mannitol (pH 7.4, 310–320 mosmol/l). Hypotonic external solution contained 105 CsCl, 0.5 $MgCl_2$, 1.3 $CaCl_2$, 10 HEPES, 20 D-mannitol (in mmol/l, pH 7.4, 240–250 mosmol/l). External bath solutions with different $[Cl^-]$ were prepared by equimolar substitution of CsCl with D-mannitol. For experiments on anion selectivity, the CsCl in the hypotonic bath solution was replaced by Na-X of equal concentration (where X = Cl^-, SCN^-, I^-, Br^-, F^-, methanesulphonate or gluconate). For Ca^{2+}-free experiments, 0.5 mmol/l EGTA was added into the bath solution. Osmolarity of all the solutions was measured using a freezing point osmometer (Fiske Associate).

Continuous superfusion and exchanges of external bath solutions, and the drug applications were performed using a rapid application system of Y-tube method as described elsewhere (Murase et al. 1990).

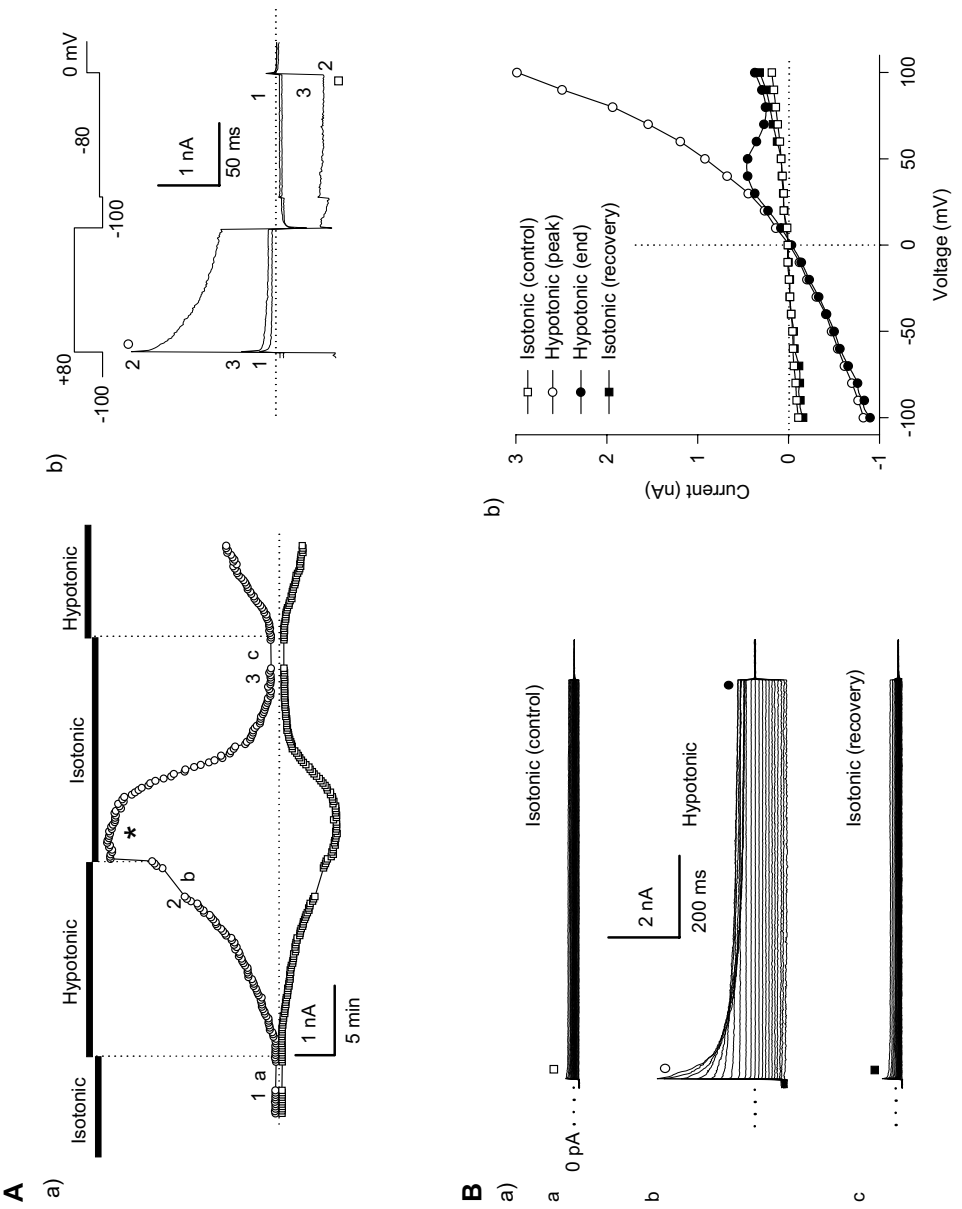

Figure 1. Activation of swelling-induced currents in a human fibroblast. **Aa.** Time course of the current activation evoked by alternate step pulses to +80 and −80 mV at 0.1 Hz from a cell exposed to isotonic and hypotonic CsCl solutions. The outward and inward current amplitude was measured at points that an open circle and an open square in Ab represent, respectively. Zero current level is indicated by a dotted line. **Ab.** Superimposed current traces recorded at points 1, 2, and 3 in Aa. Voltage protocol is shown above the traces. Command pulse to +80 mV during 100 ms was preceded by a conditioning pulse

Chemicals

All the reagents for cell culture were purchased from Gibco laboratory. NaF, methanesulphonic acid, and diphenylamine-2-carboxylic acid (DPC) were from Fluka. 5-Nitro-2-(3-phenylpropylamino)-benzoic acid (NPPB), tetrodotoxin and nimodipine were from Research Biochemical International. All other chemicals were from Sigma. Nimodipine was dissolved in ethanol to the concentration of 50 mmol/l and the other drugs were dissolved in dimethylsulfoxide. They were added to the external solution to give the appropriate concentration just before use. The vehicle alone showed a negligible effect on whole cell currents at the concentration of 0.1–0.2% ($n = 5$). All experiments with DHP drugs were carried out in dim light.

Data Analysis

The amplitudes of membrane current were measured at 5–20 ms after the start of voltage clamp steps or before the end of the pulses.

Relative anion permeabilities (P_X/P_{Cl}) were calculated from the shift in the reversal potentials (E_{rev}) following replacement of extracellular Cl^- by the anion X^- using the modified Goldman–Hodgkin–Katz equation:

$$P_X/P_{Cl} = ([Cl^-]_n \exp(-\Delta E_{rev} F/RT - Cl^-]_s)/[X^-]_s$$

where $[Cl^-]_n$ and $[Cl^-]_s$ are the Cl^- concentrations in the normal and substituted external solutions, $[X^-]_s$ is the concentration of the substituting anions, ΔE_{rev} is the shift in E_{rev}, R is the gas constant, T is absolute temperature, and F is the Faraday constant.

The half-maximal concentration (EC_{50}) values for blockers were calculated by fitting the dose-response curve to a logistic equation of the form:

$$I_{drug}/I_{control} = (1 - A)/[1 + ([drug]/EC_{50})^k] + A$$

where [drug] is the concentration of drug, A is the current value at the end of the fitting region, and k is the slope factor of the curve. A value is 0 unless stated otherwise.

All data were expressed as mean ± S.E.M. (n = number of observations), and where appropriate, tested for significance using Student's t test unless stated otherwise. Values of $P < 0.05$ were considered to be significantly different.

to −100 mV of 1 s duration. Then, brief hyperpolarization to −100 mV was followed by a −80 mV step. The cell was then held at 0 mV. **Ba.** Current traces recorded at points a (upper panel), b (center panel), and c (lower panel) in Aa. Step pulses between −100 and +100 mV for 1 s were preceded by 2 s conditioning pulse to −100 mV. An open square in a, closed and open circles in b, and a closed square in c represent the points at which the current amplitudes were measured to evaluate the I-V relationships. **Bb.** The relationships between the current magnitude and the membrane potential obtained from current traces in Ba.

Results

$I_{Cl(vol)}$ *in human fibroblasts*

When a cell was exposed to an isotonic bath solution, little currents were evoked by the alternating steps (2.7 ± 0.1 pA/pF at +80 mV, -2.6 ± 0.2 pA/pF at −80 mV, $n = 25$, Fig. 1A) and voltage-steps from −100 to +100 mV ($\Delta V = 10$ mV, Fig. 1B). The I-V relationship was slightly outward rectified (Fig. 1Bb, open squares) and E_{rev} of the currents was $+0.4 \pm 0.2$ mV ($n = 10$). Exposure of the cell to the hypo osmotic bath solution (80% osmolarity) led to a slow sizable inward and outward development of whole cell currents in response to the repetitive voltage-steps to ± 80 mV (Fig. 1A). Microscopically clearly visible cell swelling was always accompanied by the activation of the currents. The current density after 10 minutes of hypotonic exposure was -58.8 ± 6.4 and $+129.6 \pm 14.3$ pA/pF ($n = 25$) at −80 and +80 mV, respectively. The I-V relationship of the hypotonically activated current was determined using a protocol in which pulses of 1 s duration from −100 to +100 mV ($\Delta V = 10$ mV) were applied (Fig. 1B). A hyperpolarizing conditioning pulse of 2 s duration to −100 mV was applied *prior* to each command step for the recovery from a depolarization-induced inactivation (Gosling et al. 1995). The peak I-V relationship in the hypotonic condition rectified in an outward direction (Fig. 1Bb, open circles). The E_{rev} of the peak currents was $+4.7 \pm 0.6$ mV ($n = 15$), which was close to the calculated E_{Cl} (+7 mV) under the ionic condition of the experiments. A remarkable characteristic of the swelling-induced currents was a current decay during step pulses above +50 mV, which became progressively faster as the potential was clamped at increasingly positive voltages (Fig. 1Aa and Ba). This decay resulted in the cross-overs of current traces after 100–200 ms (Fig. 1Ba) and a negative slope of the end-pulse I-V relationship (filled circles in Fig. 1Bb) over the range positive to +50 mV. Upon switching from the hypotonic to the isotonic bath solution, a sudden increase in the outward currents was observed (an asterisk in Fig. 1Aa), which may be due to the increase in extracellular Cl^- concentration ($[Cl^-]_o$) from 105 to 140 mmol/l. The rise was followed by a slow reverse of the currents to the control level. Reexposing the same cells to the hypotonic bath solution caused a reactivation of the whole cell currents (Fig. 1Aa). These results show that the swelling-induced current is not a leak current or a result of cell damage during osmotic perturbation.

The swelling-induced currents were thought to be mainly selective to Cl^- because (1) pipettes and bath solutions were used with all the K^+ and Na^+ being replaced by Cs^+ (see Methods) to study the I_{Cl} in isolation from the other cationic currents, (2) E_{rev} of the currents was close to the E_{Cl} of the perfect Cl^--selective channels. To ensure it, we examined the anionic nature of the currents. Fig. 2A shows the dependence of the hypotonic-induced currents on the $[Cl^-]_o$. Voltage ramps between −120 and +120 mV were used to determine the E_{rev} of the currents in bath solutions with standard and reduced $[Cl^-]_o$. E_{rev} of the I-V relationship reconstructed from the ramp protocol ($+7.3 \pm 1.0$ mV, $n = 5$) did not

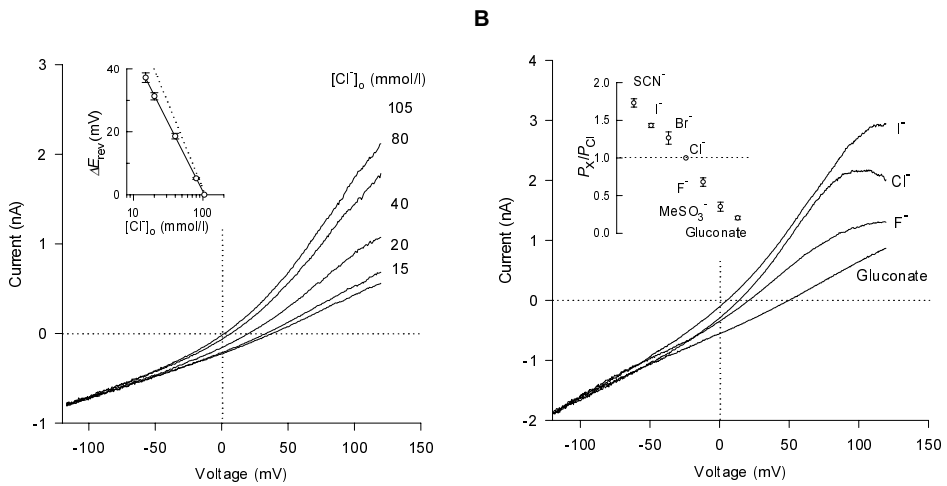

Figure 2. Cl^--dependence and anion permeability of volume-activated conductance. **A.** I-V relationships of the hypotonic-stimulated currents reconstructed from the currents measured in voltage ramps (−120 to +120 mV during 550 ms) in hypotonic solutions with 105, 80, 40, 20 and 15 mmol/l $[Cl^-]_o$. A single cell was exposed to a decreasing concentration of $[Cl^-]_o$ and data were obtained from five cells. The shift of the E_{rev} was plotted against the $[Cl^-]_o$ in inset. The solid line was derived from the linear regression for the data and the dotted line represents the expected relation for a purely Cl^--selective channel. The slope of the solid line is −44 mV/log-decade, which was close to the expected value of −54 mV/log-decade for perfect Cl^- selective channels under the experimental condition. **B.** Representative current traces from a single cell evoked by the ramp pulses in hypotonic solutions with indicated anions. Inset shows the relative permeabilities of test anions to Cl^- which was obtained from five to seven cells.

differ significantly from that obtained from the voltage-step protocol ($+4.7 \pm 0.6$ mV, $P > 0.2$). The E_{rev} of the current was shifted to depolarized potentials when the cell was exposed to decreasing $[Cl^-]_o$ (Fig. 2A), which means that the E_{rev} of the swelling-induced current is governed by the $[Cl^-]_o$ in bath solution.

To further characterize the swelling-activated conductance, we investigated anion selectivity of the channels. The swelling-activated currents were evoked by the voltage-ramp pulses in normal, hypotonic Cl^--containing external solution, and in solutions with test anions replacing Cl^- (Fig. 2B). Since the E_{rev} with NaCl in the bath ($+7.2 \pm 1.9$ mV, $n = 7$) was not significantly different from that with CsCl ($+6.0 \pm 0.9$ mV, $n = 10$, $P > 0.3$), a cationic conductance might contribute little to the currents. The anion permeabilities relative to Cl^- were calculated from the shifts in E_{rev} using the Goldman–Hodgkin–Katz equation as described in Methods. An apparent selectivity sequence for the volume-activated channels was as follows: $SCN^- > I^- \geq Br^- > Cl^- > F^-$ methanesulphonate > gluconate (Fig. 2B, Table 1), which is identical to the one described for $I_{Cl(vol)}$ in many cell types (Kubo and Okada 1992; Gosling et al. 1995). These results demonstrate that the ion channels

Table 1. Relative anion permeability (P_X/P_{Cl}) of the $I_{Cl(vol)}$

Anion	E_{rev} (mV)	P_X/P_{Cl}	n
SCN^-	-6.4 ± 2.4	1.73 ± 0.05	5
I^-	-0.3 ± 0.8	1.43 ± 0.02	5
Br^-	3.8 ± 0.9	1.26 ± 0.08	7
F^-	17.5 ± 3.4	0.68 ± 0.06	5
$MeSO_3^-$	33.7 ± 3.4	0.35 ± 0.06	5
Gluconate	47.7 ± 3.2	0.20 ± 0.02	5

E_{rev}, reversal potential; P_X/P_{Cl}, permeability ratio of ion X with respect to Cl^-; n, number of cells.

responsible for the swelling-induced currents are anion, rather than cation-selective, and indicate certain permeability to some organic anions.

Pharmacology of $I_{Cl(vol)}$

We investigated the pharmacological properties of the volume-activated conductances. The swelling-induced currents were not significantly affected by cationic channel blockers such as 1 μmol/l TTX ($1.4 \pm 0.4\%$ at +80 mV, $n = 3$) and 100 μmol/l verapamil ($2.3 \pm 0.3\%$ at +80 mV, $n = 5$). However, classical Cl^- channel blockers suppressed the current effectively. 4,4'-Diisothiocyanato-stilbene-2,2'-disulfonic acid (DIDS), a stilbene-derivative Cl^- channel blocker, inhibited $I_{Cl(vol)}$ in a dose-dependent manner (Fig. 3). The inhibitory effect of DIDS was very fast and fully reversible after washout at the concentration below 400 μmol/l (Fig. 3Aa). Blockade produced by DIDS was voltage-dependent, and the outward currents were substantially more sensitive than the inward currents (Fig. 3, Table 2). At the concentration of 1 mmol/l (the largest concentration we tested) DIDS inhibited the peak currents by $86.2 \pm 2.4\%$ and $35.4 \pm 4.9\%$ at +80 and −80 mV, respectively. Since the rate of the depolarization-induced decay of the current was accelerated in the presence of DIDS as shown in Fig. 3Ab, the efficacy of the drug on the outward currents was underestimated when the blocking effect was evaluated at the peak of the current. The inhibitory effects of DIDS, therefore, were calculated from the ratio of the total area of the currents obtained from the integration of the positive whole-cell currents before and after application of the

Figure 3. Voltage-dependent block of $I_{Cl(vol)}$ by DIDS. **Aa.** Time course of $I_{Cl(vol)}$ inhibition during sequential application of increasing concentrations of DIDS. Currents were elicited as in Fig. 1A. Open circles and squares represent the peak current amplitudes and the normalized area of the outward currents, respectively. **Ab.** Superimposed current traces recorded before and after the application of DIDS. The a, b, c, d, e and f represent the location in Aa at which the current traces were derived from. **Ba.** Current traces

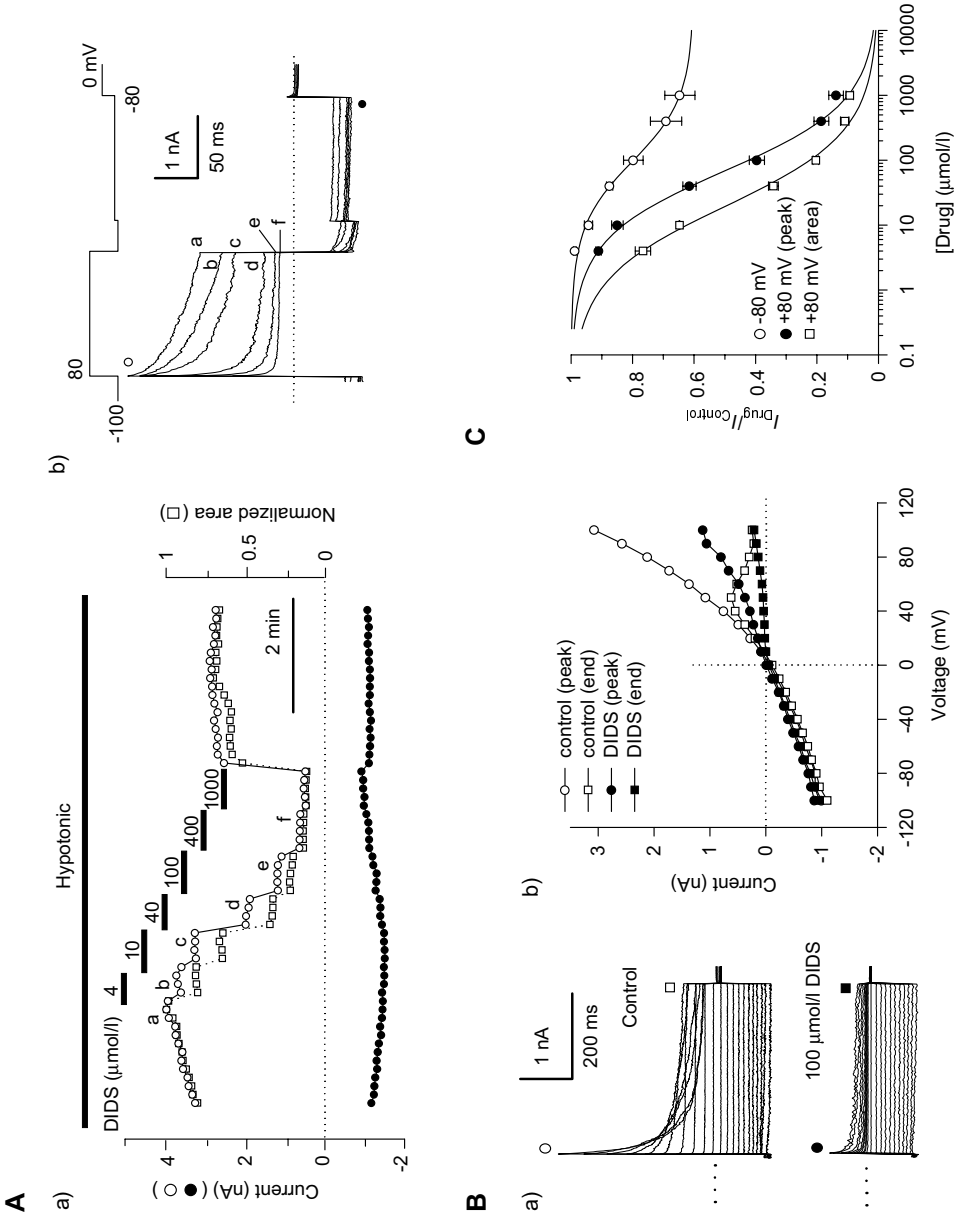

evoked by step pulses to test potentials from −100 to +100 mV before and after the application of 100 μmol/l DIDS. **Bb.** I-V plots derived from the current traces in panel Ba. **C.** Dose-response relation of DIDS on inward $I_{Cl(vol)}$ (at −80 mV, open circles), peak outward $I_{Cl(vol)}$ (at +80 mV, closed circles), and area of outward $I_{Cl(vol)}$ (at +80 mV, open squares). Each symbol represents the mean ± S.E.M. obtained from three experiments. Smooth curves were derived from the curve fit to a logistic equation from which EC_{50} values were derived.

Table 2. Pharmacology of $I_{Cl(vol)}$

Drugs		Blockade (%) or concentration (μmol/l) $V_m = +80$ mV	$V_m = -80$ mV	n
DIDS	40 μmol/l peak	38.5 ± 2.2%	12.5 ± 1.0%	
	40 μmol/l area	65.8 ± 1.6%		
	100 μmol/l peak	60.4 ± 2.5%	20.2 ± 3.2%	3
	100 μmol/l area	79.6 ± 0.9%		
	EC_{50} peak	56.7 ± 1.0 μmol/l] –*–	99.7 ± 12.5 μmol/l[#]	
	EC_{50} area	19.4 ± 1.0 μmol/l] *		
NPPB	50 μmol/l	42.9 ± 7.6%	48.7 ± 9.9%	
	100 μmol/l	78.9 ± 4.3%	81.3 ± 4.9%	5
	EC_{50}	59.0 ± 7.4 μmol/l –≈–	59.5 ± 8.5 μmol/l	
DPC	300 μmol/l	32.4 ± 4.2%	35.3 ± 5.1%	3
Nimodipine	40 μmol/l	15.1 ± 0.6%	14.0 ± 0.5%	
	100 μmol/l	84.1 ± 3.1%	85.8 ± 3.4%	6
	EC_{50}	65.7 ± 2.5 μmol/l –≈–	65.8 ± 2.8 μmol	
Nifedipine	100 μmol/l	34.9 ± 6.1%	31.0 ± 11.5%	
	200 μmol/l	67.9 ± 3.3%	67.3 ± 0.7%	
	EC_{50}	138.6 ± 1.4 μmol/l –≈–	142.6 ± 15.5 μmol/l	

[#]A value in a logistic equation was 0.6±0.04 (see open circles in Fig. 3C). * $P < 0.05$, ≈ not significantly different.

drug (Fig. 3Aa, open squares). This resulted in the significant left shift of EC_{50} value by about 38 μmol/l from 57 μmol/l to 19 μmol/l (Fig. 3C, Table 2).

NPPB, a carboxylate analogue Cl^- channel blocker also inhibited the $I_{Cl(vol)}$ reversibly. The effects of NPPB were voltage-independent (Fig. 4A,B) and the EC_{50} was ~60 μmol/l (Fig. 4C, Table 2). NPPB did not affect the inactivating property of the outward I_{Cl} (Fig. 4). Another carboxylate analogue, DPC, also inhibited the currents in the same manner as NPPB. However, the efficacy was far less than that of NPPB (Fig. 4C, Table 2).

Effects of Nimodipine

DHP, including nimodipine and nifedipine, show a selective inhibition on L-type Ca^{2+} channels at the concentration of 1–10 μmol/l in neurons and muscle cells. At that concentration, however, $I_{Cl(vol)}$ was little affected by nimodipine (1.0 ± 1.5% at +80 mV by 10 μmol/l, $n = 6$). At 100 μmol/l, nimodipine eliminated 84.1 ± 3.1% and 85.8 ± 3.4% at +80 and −80 mV, respectively, and the effect was reversible after washout of the drug (Fig. 5). The blocking characteristics of

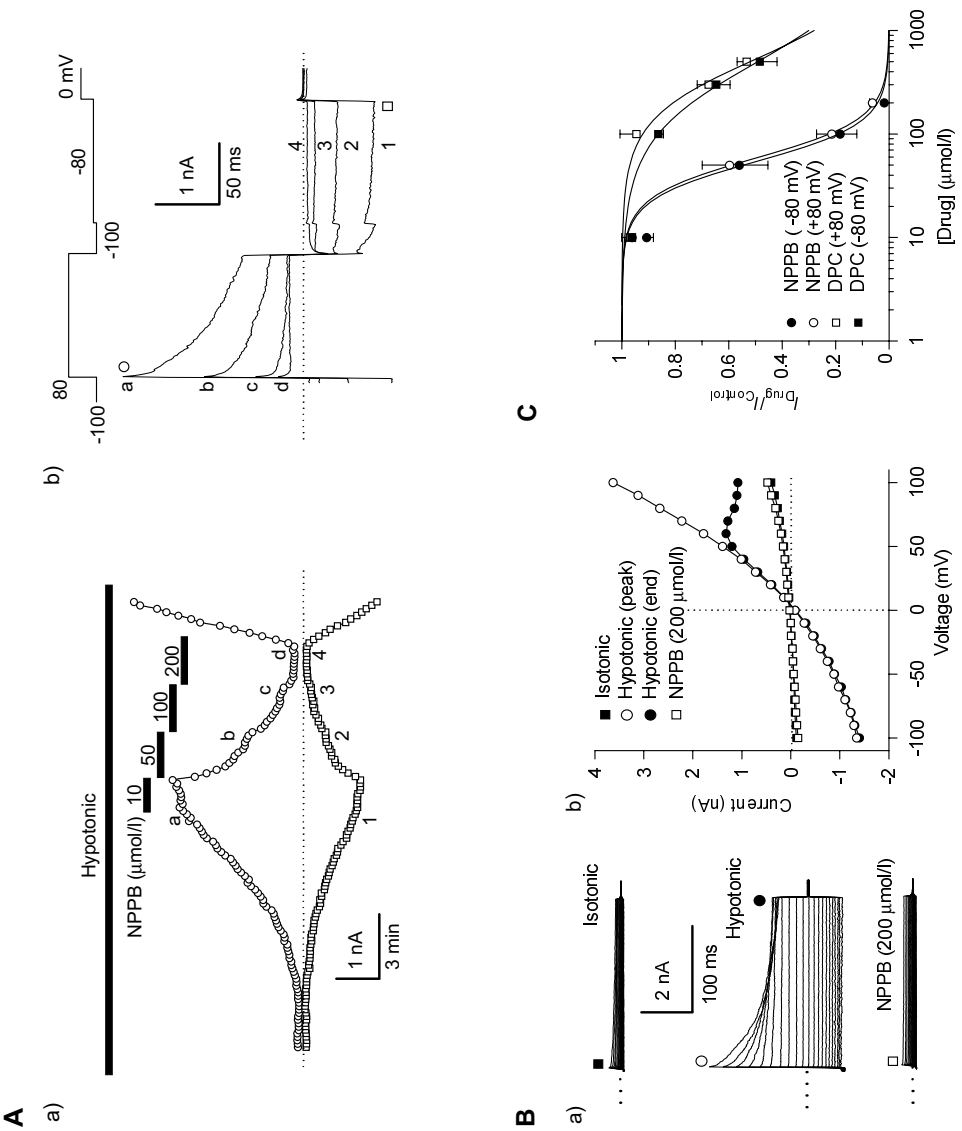

Figure 4. Inhibitory effects of NPPB on $I_{Cl(vol)}$. **Aa.** Outward (open circles) and inward (open squares) current amplitudes, evoked by the same protocol as in Fig 1A, were plotted against time. NPPB of increasing concentration eliminated the currents in a dose-dependent manner. **Ab.** Superimposed current traces recorded before and after the application of NPPB at the location indicated in Aa. **Ba.** Current traces evoked by step pulses to test potentials from −100 to +100 mV in isotonic, hypotonic solution and in the presence of 200 μmol/l NPPB. **Bb.** I-V plots derived from the current traces in Ba. **C.** Dose-dependent and voltage-independent inhibition of carboxylate-analogues, NPPB (circles) and DPC (squares) at +80 (open symbols) and −80 mV (closed symbols). Each point represents mean ± S.E.M. value derived from five (NPPB) and three (DPC) cells.

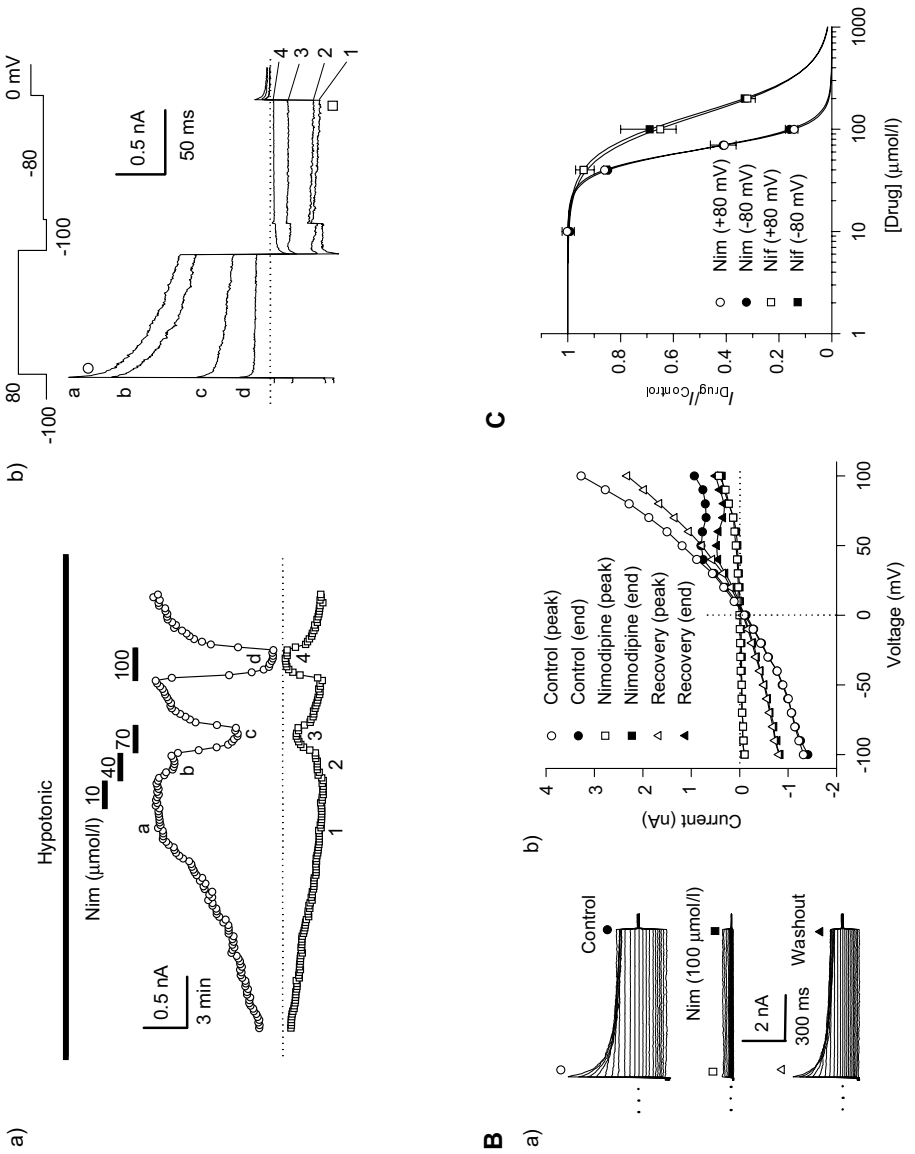

Figure 5. Potent blockade of $I_{\mathrm{Cl(vol)}}$ by nimodipine. **Aa.** Time course of $I_{\mathrm{Cl(vol)}}$ inhibition during a sequential application of 10, 40, 70, and 100 μmol/l nimodipine (Nim). **Ab.** Superimposed current traces before (a, 1) and after (b, c, d and 2, 3, 4) the superfusion of nimodipine. Symbols represent the location at which the current amplitude plotted in Aa was measured. **Ba.** Current traces evoked by step pulses between -100 and $+100$ mV before (upper), and after (middle) the application of 100 μmol/l nimodipine. Lower traces were recorded after washout of the drug during 2 min. **Bb.** I-V plots derived from the current traces in Ba. **C.** Dose-dependent and voltage-independent inhibition by nimodipine (circles, $n = 6$) and nifedipine (squares, $n = 3$).

nimodipine were quite similar to those of NPPB, and the EC_{50} was ~65 μmol/l at ± 80 mV (Fig. 5C, Table 2), which was comparable to those of NPPB (Fig. 4C). Nifedipine also showed similar blockade to nimodipine with less efficacy. At 200 μmol/l (the highest concentration we tested) nifedipine suppressed the currents by ~70% (Fig. 5C, Table 2). Although the concentration-response relationship was incomplete, estimated EC_{50} value was ~140 μmol/l (Table 2).

To determine whether the inhibition of $I_{Cl(vol)}$ by nimodipine was mediated by its Ca^{2+} channel blocking effect, we attempted to remove external Ca^{2+} from bath solution using the chelator EGTA (0.5 mmol/l), and to block the voltage-dependent Ca^{2+} channels using inorganic Ca^{2+} channel blocker Cd^{2+} (0.5 mmol/l) subsequent to the application of nimodipine. The divalent cations are reported to block the pore of the channels and affect the magnitude and kinetics of the $I_{Cl(vol)}$ (Voets et al. 1997). However, since the effects of Ca^{2+} (1.3 mmol/l) removal (Δ in Fig. 6A) and the 500 μmol/l Cd^{2+} addition (∇ in Fig. 6A) were less than ± 10% in current magnitude (9.2 ± 4.0% and -6.5 ± 4.3%, respectively, at +80 mV, $n = 4$), the current amplitude measured in the absence of nimodipine or in the presence of Cd^{2+} were regarded as a respective control to evaluate the blocking effects of nimodipine. Under those conditions, the inhibition by nimodipine was not significantly changed (Table 3, Fig. 6A), suggesting the Ca^{2+}-independent blockade of $I_{Cl(vol)}$ by nimodipine.

Table 3. Ca^{2+}-independence of nimodipine blockade on $I_{Cl(vol)}$

	Blockade by 100 μmol/l nimodipine (%)		n
	$V_m = +80$ mV	$V_m = -80$ mV	
Control	83.6 ± 1.8	86.3 ± 1.7	10
External 0 mmol/l Ca^{2+}, 0.5 mmol/l EGTA	85.7 ± 2.3	88.4 ± 2.6	4
External 0.5 mmol/l Cd^{2+}	81.4 ± 4.4	84.4 ± 2.6	4

No data were significantly different from the control value when investigated by analysis of variance ($P > 0.7$).

Discussion

$I_{Cl(vol)}$ in human fibroblasts

We showed that the currents activated by hypotonic cell swelling are Cl^- currents identical to the $I_{Cl(vol)}$ reported in many other preparations (Kubo and Okada 1992; Gosling et al. 1995; Nilius et al. 1997). Our conclusion is based on the following observations: (1) the currents were recorded in the presence of internal and external Cs^+ replacing internal K^+ and external Na^+, a condition under which Cl^- was the major permeant ion, (2) the E_{rev} of the currents was close to the predicted

E_{Cl} and was shifted as the $[Cl^-]_o$ changed (Fig. 2A), (3) the replacement of external Cl^- by less permeable anions greatly reduced the outward currents (Fig. 2B), (4) the currents were sensitive to classical Cl^- channel blockers, DIDS (Fig. 3), NPPB and DPC (Fig. 4), and (5) several kinetic properties, such as outwardly rectifying I-V relationship and depolarization-induced inactivation were identical to those described for volume-activated Cl^- channels. Fibroblastic cells (Rugolo et al. 1989; Mastrocola et al. 1991; Mastrocola et al. 1993) including human fibroblasts from periodontal ligament (Bibby and McCulloch 1994) were reported to show RVD in response to hypotonic cell swelling. In fibroblasts, the activation of separate conductive K^+ and Cl^- pathway, rather than ion exchanging systems such as Cl^-/HCO_3^- or K^+/H^+ was suggested to be the important mechanism involved in the loss of internal KCl (Rugolo et al. 1989; Mastrocola et al. 1991; Mastrocola et al. 1993). In addition, the Cl^- conductances are more enhanced than those of K^+ in the volume regulation (Mastrocola et al. 1991) suggesting the importance of the functional role of a volume-sensitive Cl^- pathway in the RVD of the fibroblasts. Although we did not bring the direct evindence for the role of $I_{Cl(vol)}$ in the present study, the channels may participate in the RVD response in human fibroblasts.

Effects of nimodipine

We expected the underlying mechanism of the Ca^{2+}-independent nimodipine blockade of RVD and osmolyte efflux (Sánchez-Olea et al. 1995; Morán et al. 1997a,b; Pasantes-Morales et al. 1997) to be associated with $I_{Cl(vol)}$ because of the well-known characteristics of the channels, i.e. a permeability to the organic osmolytes and Cl^- during RVD, and a Ca^{2+}-independent activation (Nilius et al. 1996). In our study $I_{Cl(vol)}$ from human fibroblasts also showed a significant permeability to gluconate ($\sim$0.2, Table 1), and were activated in the condition of internal 0 mmol/l Ca^{2+}/1 mmol/l EGTA.

As expected, nimodipine efficiently suppressed the $I_{Cl(vol)}$. The effects were reversible after washout and dose-dependent with a similar potency to those of NPPB (Fig. 5, Table 2). There are several possible mechanisms whereby nimodipine can achieve its blocking effects on $I_{Cl(vol)}$. First, nimodipine is a well-known DHP Ca^{2+} channel blocker. By blocking the channels, Ca^{2+} influx is diminished, and thereby activation of $I_{Cl(vol)}$ is reduced. However, this is unlikely action of nimodipine under our conditions for three reasons: (1) the effects of nimodipine did not change under external Ca^{2+}-free condition (external 0 mmol/l Ca^{2+}/0.5 mmol/l EGTA) and in the presence of an inorganic Ca^{2+} channel blocker Cd^{2+} (Fig. 6A), (2) the inhibitory concentration was much higher than that required for blocking the L-type Ca^{2+} channels (Fig. 5), and (3) verapamil (100 μmol/l), another Ca^{2+} channel blocker, did not show any significant inhibitory effect. These findings demonstrate that the effects of nimodipine are not mediated by the inhibition of voltage-dependent Ca^{2+} channels. Although the mechanism of the blockade by nimodipine on the volume-activated Cl^- channels is unclear, it may modulate the gating process of the channels, e.g. produce a shift of voltage-dependence of gating as NPPB does (Alton and Williams 1992), rather than act as a channel

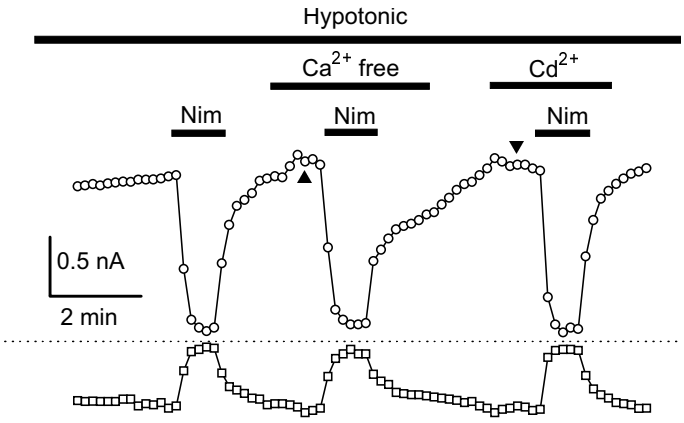

Figure 6. Ca^{2+}-independent blockade of $I_{Cl(vol)}$ by nimodipine. Time course of inhibition of $I_{Cl(vol)}$ by the extracellular superfusions with 100 μmol/l nimodipine, and the lack of effects of Ca^{2+} removal (0 mmol/l Ca^{2+}/0.5 mmol/l EGTA) and Cd^{2+} addition (0.5 mmol/l) on nimodipine blockade.

blocker as in the case of DIDS. However, single-channel studies are required to clarify the precise mechanism.

These effects of nimodipine on $I_{Cl(vol)}$ is likely to be applied to other DHP blockers because nitrendipine was also reported to suppress the RVD responses and efflux of osmolytes with potency similar to nimodipine (Sánchez-Olea et al. 1995; Morán et al. 1997b). In this experiment, the effects of nifedipine on $I_{Cl(vol)}$ were tested, which were found identical to those of nimodipine, i.e. Ca^{2+}-independent blockade, except its weak potency (Figs. 6C and 7B).

In conclusion, $I_{Cl(vol)}$ is activated by hypotonic cell swelling in human fibroblasts and a DHP-Ca^{2+} channel blocker nimodipine inhibited the currents in an extracellular Ca^{2+}-independent way. This may account for, at least in part, the Ca^{2+}-independent suppressive effects of nimodipine on RVD response and Cl^-/organic osmolytes efflux under hypotonic condition reported in several preparations (Sánchez-Olea et al. 1995; Morán et al. 1997a,b; Pasantes-Morales et al. 1997). In addition, although the molecular identity of the volume-activated Cl^- channels and its similarity to that of DHP-sensitive Ca^{2+} channels are unclear, it is interesting that the Cl^- channel blocker NPPB inhibited L-type Ca^{2+} channels in smooth muscle myocytes (Doughty et al. 1998), and that mibefradil, a novel Ca^{2+} channel antagonist, suppressed $I_{Cl(vol)}$ efficiently in endothelial cells (Nilius et al. 1997).

Acknowledgements. The authors wish to thank Dr. In-Seok Lee for help with the cell culture and his valuable advice. The assistance of Mi-Hyun Lew throughout the experiments is appreciated.

References

Alton E. W., Williams A. J. (1992): Modification of gating of an airway epithelial chloride channel by 5-nitro-2-(3-phenylpropylamino) benzoic acid (NPPB). J. Membr. Biol. **128**, 141—151

Bibby K. J., McCulloch C. A. (1994): Regulation of cell volume and $[Ca^{2+}]_i$ in attached human fibroblasts responding to anisosmotic buffers. Am. J. Physiol. **266**, C1639—1649

Doughty J. M., Miller A. L., Langton P. D. (1998): Non-specificity of chloride channel blockers in rat cerebral arteries: block of the L-type calcium channel. J. Physiol. (London) **507**, 433—439

Gosling M., Smith J. W., Poyner D. R. (1995): Characterization of a volume-sensitive chloride current in rat osteoblast-like (ROS 17/2.8) cells. J. Physiol. (London) **485**, 671—682

Hamill O. P., Marty A., Neher E., Sakmann B., Sigworth F. J. (1981): Improved patch-clamp techniques for high-resolution current recording from cells and cell-free membrane patches. Pflügers Arch. **391**, 85—100

Kubo M., Okada Y. (1992): Volume-regulatory Cl^- channel currents in cultured human epithelial cells. J. Physiol. (London) **456**, 351—371

Mastrocola T., Flamigni A., Rugolo M. (1991): Hypotonic shock activated Cl^- and K^+ pathways in human fibroblasts. Biochim. Biophys. Acta **1069**, 201—208

Mastrocola T., Lambert I., Kramhøft H., Rugolo M., Hoffmann E. K. (1993): Volume regulation in human fibroblasts: Role of Ca^{2+} and 5-lipoxygenase products in the activation of the Cl^- efflux. J. Membr. Biol. **136**, 55—62

Moran J., Miranda D., Pena-Segura C., Pasantes-Morales H. (1997a): Volume regulation in NIH/3T3 cells not expressing P-glycoprotein. II. Chloride and amino acid fluxes. Am. J. Physiol. **272**, C1804—1809

Moran J., Morales-Mulia S., Hernandez-Cruz A., Pasantes-Morales H. (1997b): Regulatory volume decrease and associated osmolyte fluxes in cerebellar granule neurons are calcium independent. J. Neurosci. Res. **47**, 144—154

Murase K., Randic M., Shirasaki T., Nakagawa T., Akaike N. (1990): Serotonin suppresses N-methyl-D-aspartate responses in acutely isolated spinal neurons of the rat. Brain Res. **525**, 84—91

Neher E. (1992): Correction for liquid junction potentials in patch clamp experiments. Methods Enzymol. **207**, 123—131

Nilius B., Eggermont J., Voets T., Droogmans G. (1996): Volume-activated Cl^- channels. Gen. Pharmacol. **27**, 1131—1140

Nilius B., Prenen J., Kamouchi M., Viana F., Voets T., Droogmans G. (1997): Inhibition by mibefradil, a novel calcium channel antagonist, of Ca^{2+} and volume-activated Cl^- channels in macrovascular endothelial cells. Br. J. Pharmacol. **121**, 547—555

O'Connor E., Kimelberg H. K. (1993): Role of calcium in astrocyte volume regulation and in the release of ions and amino acids. J. Neurosci. **13**, 2638—2650

Okada Y. (1997): Volume expansion-sensing outward-rectifier Cl^- channel: fresh start to the molecular identity and volume sensor. Am. J. Physiol. **273**, C755—789

Pasantes-Morales H., Sanchez-Olea R., Miranda D., Moran J. (1997): Volume regulation in NIH/3T3 cells not expressing P-glycoprotein. I. Regulatory volume decrease. Am. J. Physiol. **272**, C1798—1803

Rugolo M., Mastrocola T., Flamigni A., Lenaz G. (1989): Chloride transport in human fibroblasts is activated by hypotonic shock. Biochem. Biophys. Res. Commun. **154**, 719—726

Sánchez-Olea R., Mulia M. M., Morán J., Pasantes-Morales H. (1995): Inhibition by dihydropyridines of regulatory volume decrease and osmolyte fluxes in cultured astrocytes is unrelated to extracellular calcium. Neurosci. Lett. **193**, 165—168

Somerman M. J., Foster R. A., Imm G. M., Sauk J. J., Archer S. Y. (1989): Periodontal ligament cells and gingival fibroblasts respond differently to attachment factors *in vitro*. J. Periodontol. **60**, 73—77

Voets T., Droogmans G., Nilius B. (1997) Modulation of voltage-dependent properties of a swelling-activated Cl^- current. J. Gen. Physiol. **110,** 313—325

Final version accepted: April 11, 2001